Biology Direct

RESEARCH Open Access

Deciphering the impact of MreB on the morphology and pathogenicity of the aquatic pathogen *Spiroplasma eriocheiris*

Rong Li[1†], Xiaohui Cao[2†], Jiaxin Chen[1†], Tingting He[3†], Yan Zhang[1], Wen Wang[4], Yaqi Wang[1], Yifei Wang[1], Yanyan Qiu[1], Mengji Xie[1], Kailin Shi[1], Yuhua Xu[1], Siyuan Zhang[1] and Peng Liu[1*]

Abstract

Background *Spiroplasma eriocheiris* has been proved to be a pathogen causing tremor disease of *Eriocheir sinensis*, it is also infectious to other aquatic crustaceans, resulting in a serious threat on the sustainable development of the aquaculture industry. *S. eriocheiris* is a helical-shaped microbe without a cell wall, and its motility is related to the cytoskeleton protein MreB which belongs to the actin superfamily and has five MreB homologs.

Results In this study, we purified MreB3, MreB4 and MreB5, and successfully prepared monoclonal antibodies. After *S. eriocheiris* treated with actin stabilizator Phalloidin and inhibitors A22, we found that Phalloidin and A22 affect the *S. eriocheiris* morphology by altering MreB expression. We confirmed that the ability of *S. eriocheiris* to invade *E. sinensis* was increased after treatment with Phalloidin, including that the morphology of *E. sinensis* blood lymphocytes was deteriorated, blood lymphocytes viability was decreased, peroxidase activity and cell necrosis were increased. On the contrary, the pathogenicity of *S. eriocheiris* decreased after treatment with A22.

Conclusions Our findings suggest that the MreB protein in *S. eriocheiris* plays a crucial role in its morphology and pathogenicity, providing new insights into potential strategies for the prevention and control of *S. eriocheiris* infections.

Keywords A22, MreB, Pathogenicity and morphology, Phalloidin, *Spiroplasma eriocheiris*

Background

Spiroplasma was first discovered in maize with dwarf disease by Robert Davis, an American plant pathologist. It belongs to the taxonomic groups *Mollicutes*, *Entomoplasmatales* and *Spiroplasmataceae*. Like other members of *Mollicutes*, *S. eriocheiris* is characterized by its absence of a cell wall [1, 2], has a diameter of about 0.1–0.2 μm, and it can pass through a filter membrane with a pore size of 0.22 μm. The vast majority of *Spiroplasma* species identified to date have been isolated from insects and terrestrial plants, where they commonly exhibit parasitic behavior within host cells. Over the course of their long-term evolution, these bacteria have established three

†Rong Li, Xiaohui Cao, Jiaxin Chen and Tingting He contributed equally to this work.

*Correspondence:
Peng Liu
pengliu@live.cn
[1]Institute of Pathogenic Biology, Basic Medical School,University of South China, Hunan Provincial Key Laboratory for Special Pathogens Prevention and Control, Hengyang, Hunan 421001, China
[2]Jiangsu Marine Fisheries Research Institute, Nantong, Jiangsu 226007, China
[3]Shaoxing Center for Disease Control and Prevention, 276 Century Street, Shaoxing, Zhejiang Province 312000, China
[4]Jiangsu Key Laboratory for Biodiversity and Biotechnology, Jiangsu Key Laboratory for Aquatic Crustacean Diseases, College of Life Sciences, Nanjing Normal University, Jiangsu, China

distinct relationships with their hosts parasitism, symbiosis, and pathogenicity [3]. "Trembling disease" is one of the most serious epidemic diseases of *E. sinensis*, which causes huge economic losses to the aquaculture industry [4–6]. There is a research team isolated and cultivated the pathogen that causes the disease, they designated it as *S. eriocheiris* [7], this discovery challenged the previous notion that *Spiroplasma* exclusively infects terrestrial plants and insects, thus expanding our understanding of its host range from land to water for the first time [8]. In recent years, *S. eriocheiris* has also been found in aquatic crustaceans such as *M. rosenbergii*, *P. clarkii*, and *M. nipponense* [8–10]. In addition, researchers have isolated a strain of bacteria that is phylogenetically related to *S. eriocheiris* from blood cultures of Chinese patients who developed a lung infection after surgery. This result shows that *S. eriocheiris* not only harms aquaculture industry, but also may pose a threat to human health [11].

The morphology of *S. eriocheiris* is variable due to the absence of a cell wall, exhibiting different forms during various growth stages. Despite lacking flagella or cilia, *S. eriocheiris* can still rely on its cytoskeleton for movement. The cytoskeleton not only maintains the helical morphology of *S. eriocheiris*, but also functions as a motor that directly powers its movement [12, 13]. Previously, it was believed that cytoskeletons were exclusive to eukaryotes. In eukaryotes, the cytoskeleton encompasses the cytoplasmic network composed of three protein components, including microtubules, microfilaments, and intermediate filaments. However, recent studies have revealed their presence in prokaryotes such as bacteria. To date, the bacterial proteins FtsZ, MreB, and CreS have been identified as counterparts of tubulin, actin, and intermediate filament in eukaryotic cell cytoskeleton proteins, respectively. These proteins play crucial roles in cellular processes such as cell division, morphological maintenance and regulation [14]. The cytoskeleton protein MreB, among the three cytoskeleton proteins discovered in bacteria, has been identified in numerous bacterial species [15], including *Bacillus subtilis*, *Thermus thermophiles*, *Escherichia coli*, *Myxococcus xanthus* and so on. The study showed that the *S. eriocheiris* genome contains five to seven MreB homologs, each of which is an independent replicate and has a different function [13, 16]. MreB polymerizes into non-helical filaments with juxtaposed subunits, in which two filaments interact and are inverted parallel [17]. It was demonstrated that the structure of MreB and fibril is crucial in the movement of *S. citri* [18], the MreB polymer structure coordinates fibril to maintain helicity produce kinking motions [19]. Due to its distinctive helical structure and locomotion mechanism, *S. eriocheiris* is widely recognized as a highly appealing model organism for international research [20]. The helical shape of *S. eriocheiris* is maintained by the cytoskeleton within its cells, which also serves as the propulsive force driving its movement and preserving its helical morphology [21]. In recent years, numerous scholars have conducted preliminary investigations on the cytoskeleton and motility of *S. eriocheiris.* The MreB proteins constitute a significant portion of the cell cytoskeleton in *S. eriocheiris*, with five subtypes identified [22]. Among these proteins, four MreB proteins (MreB1, MreB2, MreB4, and MreB5) have been characterized in the genome of *S. eriocheiris*, demonstrating their crucial role in maintaining cellular morphology and motility [13]. *S. eriocheiris* exhibited a typical helical shape during the logarithmic growth period, while during the decay period, it displayed a spherical shape (Unpublished data). The transcription of the five MreB genes differed significantly between these two phenotypes (unpublished data), indicating that MreB is closely associated with the phenotype of *S. eriocheiris*.

A22(S-(3,4-dichlorobenzoyl) isothiourea) is a derivative of S-benzoyl isothiourea, it was discovered during a randomized screening of *E. coli* chromosome assignment inhibitors using the nucleophile blue test [23, 24]. The compound A22 is a reversible, competitive inhibitor of the actin-like protein MreB that can induce changes in cell shape, division defects and irregular segregation of chromosome in *E. coli* and *Caulobacter crescentus* [14]. The A22 was first shown to induce the formation of spherical cells in *E. coli* [25]. Several studies have demonstrated that A22 disrupts the rod-like structure of bacterial cells by interacting with MreB, resulting in a transition from a rod-like to a spherical shape [26–28]. Phalloidin is a bicyclic heptapeptide originally isolated from the death cap mushroom *Amanita phalloides* and is well known for its ability to bind stochiometricly to F-actin [29]. It binds to actin filaments much more tightly than to actin monomers and shifts the equilibrium between filaments and monomers toward filaments [30]. The investigation into the cytoskeleton proteins of *S. eriocheiris* is still in its nascent stage, and the findings have established a robust groundwork for subsequent research on the cytoskeleton of *S. eriocheiris.*

In this study, we localized MreB in *S. eriocheiris* and successfully observed the effects of Phalloidin and A22 on the morphology of *S. eriocheiris*, examined the changes in the expression of MreB in response to treatment with Phalloidin and A22, and investigated the effects of Phalloidin and A22 on the pathogenicity of *S. eriocheiris*.

Materials and methods

Monoclonal antibody preparation of MreB

Five specific peptides of MreB were sent to the company for chemical synthesis and preparing specific monoclonal antibodies, the specific sequences of the five chemically synthesized MreB are shown in Table 1. After the

Table 1 Sequences of MreB to prepare monoclonal antibodies

No.	Name	Start	End	Sequences
1	Mreb1	1	14	MALINNKKPTFVSI
2	Mreb2	252	265	VMIKPEEIKNVLLA
3	Mreb3	337	350	EKEIRDRLIEENKK
4	Mreb4	355	368	DILRQEQMHTKELD
5	Mreb5	327	340	RKRIENGYYNFNDK

monoclonal antibody was prepared, the effect of the antibody was detected by Western Blot. The logarithmic phase of *S. eriocheiris* was crushed by a cell crusher, and then the prepared protein samples were subjected to SDS-PAGE gel electrophoresis. PVDF membranes and four sheets of filter paper of appropriate size were cut and equilibrated in the transfer buffer, and then placed in the order of filter paper, gel, PVDF membrane and filter paper, and the transfer was carried out at 80 V. After the membrane transfer, the PVDF film were blocked with 5% skim milk for 2 h, washed with TBST, and then incubated at 4 °C overnight with MreB3, MreB4, MreB5 and the reference SPE-0313 primary antibody. Finally, HRP-conjugated anti-mouse IgG (H+L) was added, and the mixture was incubated at room temperature for 2 h. The proteins were detected with the high-sensitivity ECL chemiluminescence kit. Finally, MreB3, MreB4 and MreB5 were all detected at the corresponding locations (Figure. S1), while MreB1 and MreB2 had no specific bands and their monoclonal antibodies were unavailable, MreB3, MreB4 and MreB5 antibodies were successfully prepared and had good specificity, which was sufficient to meet the needs of downstream experiments.

Observation on the morphology and cytoskeleton of *S. eriocheiris* in buffer and H_2O

S. eriocheiris inoculated were observed under a phase contrast microscope to ensure that they were not contaminated with stray bacteria. The *S. eriocheiris* reached logarithmic stage was centrifuged and then suspended with PBS and H_2O respectively, phase contrast microscope was applied to observe and photograph. *S. eriocheiris* was collected and resuspended with PBS, the resuspended *S. eriocheiris* was dripped onto a copper mesh and kept at room temperature for 10 min. Finally, 1% ammonium molybdate was used for negative dyeing for 1 min. After the excess dyeing solution was removed, the samples were put into an electronic drying oven overnight for observing morphology under electron microscope. *S. eriocheiris* was treated with the same manner as described above. Triton X-100 was dropped onto the copper mesh containing the sample, and the excess Triton X-100 immediately was sucked off with filter paper, repeating this process three times. The copper mesh was washed 5 times with PBS after Triton X-100 treatment to remove the residual treatment solution. Finally, 1% ammonium molybdate was used for negative dyeing for 1 min, after absorbing excess dyeing solution, the samples were put into an electronic drying oven overnight for observing the cytoskeleton under electron microscope. *S. eriocheiris* was cultivated to logarithmic stage and suspended with PBS and H_2O. Electron microscope was used to observe the corresponding shape is helical or spherical, *S. eriocheiris* was broken by cell crusher, and the protein samples were prepared for SDS-PAGE gel electrophoresis, Refer to "Monoclonal antibody preparation of MreB" for the procedure of membrane transfer.

Detection of MreB localization using immunoelectron microscopy

The copper mesh with carbon film was irradiated under ultraviolet lamp for 30 min to increase the adsorption capacity of the copper mesh. Two mL *S. eriocheiris* in the logarithmic phase were taken, centrifuged, and resuspended with H_2O and PBS, respectively. The resuspended *S. eriocheiris* was dripped onto a copper mesh and kept at room temperature for 10 min. Making a wax disc with a candle, and then adding 3% BSA dropwise. The edge of the copper mesh was clamped with tweezers and placed upside down on the BSA. After being sealed at room temperature for 30 min, it was washed with PBST. The monoclonal antibodies to MreB3, MreB4 and MreB5 prepared by the company were used as primary antibodies. The primary antibody was taken and dripped onto the wax plate, the cleaned copper mesh was upside down on the primary antibody, and incubated at room temperature for 1 h before cleaning. Anti-rabbit IgG labeled with colloidal gold particles was used as the secondary antibody, it was mixed with PBS containing 1% BSA, and then the mixed secondary antibody was dripped onto the wax plate. The copper mesh was upside down on the secondary antibody, and the negative dyeing was performed with 1% ammonium molybdate for 1 min. Finally, the excess dye solution was absorbed with filter paper, and samples were observed under electron microscope after being put in an electronic drying oven overnight.

The observation of the morphology and cytoskeleton of *S. eriocheiris*

The copper grid is exposed to ultraviolet light to increase its adsorption capacity, *S. eriocheiris* was cultivated to the logarithmic phase with 2.5 μg/mL phalloidin and 200 μg/mL A22, then collected and re-suspended with PBS. The re-suspended *S. eriocheiris* was dripped onto a copper grid and kept at room temperature for 10 min. Triton X-100 solution is configured with PBS, it is a derivative of polyethylene glycol and was dropped onto the copper grid containing the sample, and immediately suck off the excess Triton X-100 solution with filter paper, repeat this process three times. The copper grid was washed 5

times with PBS after Triton X-100 treatment to remove the residual treatment solution. Finally, 1% ammonium molybdate was used for negative dyeing for 1 min. After absorbing excess dyeing solution, the samples were put into an electronic drying oven overnight for observation under electron microscope. The changes in MreB expression were detected by Western Blot as described above.

Quantity of *S. eriocheiris* detected using CCU method

The Phalloidin and A22 were dissolved in DMSO and sterile H_2O respectively to prepare the solution, and then the overnight cultivated *S. eriocheiris* was treated with the prepared solution. The treated *S. eriocheiris* was put in an incubator at 30 °C for 12 h, and the photos were taken after using microscopy to ensure that it was not contaminated with bacteria. After extending the cultivation time of the above *S. eriocheiris* to 8 days, three groups of *S. eriocheiris* incubated for 12 h and 8 days were taken for microscopic examination to ensure that they were not contaminated with stray bacteria. The CCU method, also called the colour change unit method, is based on the principle of detecting the relative concentration of *S. eriocheiris* by using the metabolic activity of the *S. eriocheiris* in a liquid medium. This method is usually used for microorganisms that are too small to be counted using normal turbidimetry [31]. In this experiment, a new centrifuge tube was taken from each group with *S. eriocheiris* medium, and then 100 μL of *S. eriocheiris* from each group that had been cultured for 12 h and 8 days was taken into the first centrifuge tube and mixed. 100 μL of the mixture from the first centrifuge tube was added to the second centrifuge tube and so on, until the tenth centrifuge tube. The above centrifugal tube was sealed and put into an incubator at 30 °C. The sample was taken out for microscopy examination and imaging after 12 h.

Statistics on *S. eriocheiris* mortality and *E. sinensis* survival rate

The *S. eriocheiris* cultivated with 2.5 μg/mL Phalloidin and 200 μg/mL A22 were examined by microscope to ensure that they were not contaminated with other bacteria. The *S. eriocheiris* were collected by centrifugation at 4 ℃ and 11,000 rpm for 10 min, and the supernatant was discarded. After two times centrifugation washes with pre-cooled PBS. Binding buffer, AnnexinV-FITC and PI Staining Solution were added and gently blown out respectively. Binding buffer was added after incubation for 10 min at room temperature away from light, and the stained samples were detected by flow cytometry. The *S. eriocheiris* cultivated with Phalloidin and A22 was collected and resuspended, and then divided into four groups, including R2 medium, *S. eriocheiris* group, Phalloidin treatment group and A22 treatment group. Each *E. sinensis* was injected with 100 μL of the corresponding *S. eriocheiris*, and R2 was used as a control. Finally, the circulating water system where the infected *E. sinensis* lives was heated to 28 °C, and the survival rate was counted daily.

Morphology observation of blood lymphocytes in *E. sinensis*

Six healthy *E. sinensis* were selected and their appendages were disinfected with alcohol. A total of 12 tubes of 400 μL of blood were taken in centrifuge tubes containing anticoagulant. After centrifugation, the supernatant was discarded and resuspended in L15 medium. The blood lymphocytes were added to the six-well plate and cultivated in an incubator at 28 °C for 3 to 6 h until they were adherent to the wall. Then the cells were divided into four groups, including L15, *S. eriocheiris*, *S. eriocheiris*+Phalloidin and *S. eriocheiris*+A22 group. The *S. eriocheiris* cultivated with Phalloidin and A22 was examined under a microscope to ensure that it was free of foreign bacteria. After collecting the *S. eriocheiris*, it was resuspended with L15 and added into each well of the six-well plate. The cell morphology was observed at 0, 12 and 24 h after *S. eriocheiris* infection.

Activity detection of blood lymphocytes in *E. sinensis*

The detailed procedures for the cultivation of blood lymphocytes and the *S. eriocheiris* treatment can be found in "Morphology observation of blood lymphocytes in the *E. sinensis*". To detect the activity of blood lymphocytes, the old medium was removed from the cells after morphological observation, and new medium was added, then 100 μL CCK-8 Solution was added and incubated in an incubator at 28 °C for 1 h. Finally, the absorbance at 450 nm was detected by the ELISA instrument. The culture medium in the six-well plates was removed after infection for 0, 12 and 24 h. The total DNA of blood lymphocytes was extracted according to the EasyPure Genomic DNA kit. The concentration of DNA and dilute each sample to the same concentration. The copy number of *S. eriocheiris* was detected by qRT-PCR, and finally statistical analysis was conducted by SPSS software. The blood lymphocytes were cultivated according to the same steps as above and then resuspended by centrifugation. L-dopamine and Tris-HCl were added after incubation with ultrasonic crushing, and the absorbance values were measured at 490 nm. The concentration of the broken liquid was measured by Coomassie brilliant blue protein quantitative test box. Finally, the phenoloxidase (PO) activity of blood lymphocytes was detected according to the formula for calculating PO activity.

Flow cytometry for blood lymphocytes apoptosis detection

The detailed procedures for the cultivation of blood lymphocytes and the *S. eriocheiris* treatment can be found in "Morphology observation of blood lymphocytes in the *E. sinensis*". After the cells were stained with Annexin V-FITC/PI Apoptosis Detection Kit, the apoptosis of the cells was detected by flow cytometry. Refer to "Statistics on *S. eriocheiris* mortality and *E. sinensis* survival rate" for specific operation methods.

Statistic method

Data were analyzed using SPSS 13.0 software. A t-test was used for comparison between the two groups, significant difference was determined when the P value was less than 0.05.

Results

Morphology of *S. eriocheiris* and cytoskeleton in buffer and H_2O

To observe the *S. eriocheiris* in the logarithmic stage, *S. eriocheiris* not only had a typical helical shape in the medium, but also in the PBS buffer (Fig. 1A), *S. eriocheiris* at logarithmic phase rapidly changes from helical to spherical when cells were placed in H_2O (Fig. 1B). When the PBS buffer is added back, it quickly reverts from a spherical shape to a typical helical shape. To observe the morphology of *S. eriocheiris* more clearly, *S. eriocheiris* was negatively stained and then observed by transmission electron microscope. Electron microscopy results revealed the typical helical structure of *S. eriocheiris* in the PBS buffer, with clear observation of the tip structure and tail (Fig. 1C), but appears spherical in H_2O (Fig. 1D). The cytoskeleton of *S. eriocheiris* plays an important role in its growth and morphology. Under electron microscope observation, the *S. eriocheiris* cytoskeleton in PBS was composed of dumbbell-shaped structure and a flat ribbon-like structure, (Fig. 1E), which was similar to the previous study [13], but the cytoskeleton of *S. eriocheiris* cell in the H_2O showed the round structure, which did not have dumbbell and flat ribbon structure, and only filament structures were observed (Fig. 1F).

Alteration of *S. eriocheiris* cytoskeleton protein expression in buffer and H_2O

According to the above experiments, when the morphology of *S. eriocheiris* changes, its cytoskeleton also changes accordingly. To further investigate whether the expression of the cytoskeleton protein MreB changed when the *S. eriocheiris* presented a spherical shape, quantitative western blot analysis was performed (Fig. 2A). The results of the experiment indicate that the MreB5 of helical *S. eriocheiris* was not significantly different compared with spherical *S. eriocheiris* at 0, 6 and 12 h (Fig. 2D), there was no significant difference in the expression levels of MreB3 and MreB4 in helical *S. eriocheiris* at 0 and 6 h, but they were significantly higher than spherical *S. eriocheiris* at 12 h (Fig. 2B and C).

Localization of MreB in *S. eriocheiris*

To determine whether MreB localization on the surface of *S. eriocheiris*, we incubated *S. eriocheiris* with MreB-specific antibody, and then incubated it with secondary antibody containing gold particles. After negative staining, the stained samples were observed by electron microscopy. As shown in Fig. 3, in the control group using primary antibodies labeled with His tags as a negative control, no gold particles were observed on the surface of *S. eriocheiris* (Fig. 3A). But specific primary antibodies of MreB3, MreB4 and MreB5 were presented on the surface of *S. eriocheiris*, respectively, because some gold particles were aggregated on one end of *S. eriocheiris* (Fig. 3B and D), and others were uniformly distributed on the whole surface of *S. eriocheiris* (Fig. 3C). The results revealed that the three kinds of cytoskeleton proteins were distributed in the outer membrane of *S. eriocheiris*.

The effects of Phalloidin and A22 on the morphology and MreB expression of *S. eriocheiris*

After identifying the cytoskeleton protein MreB in *S. eriocheiris*, we treated *S. eriocheiris* with the promoter Phalloidin and the specific inhibitor A22, and the morphology was observed by transmission electron microscopy after negative staining. As shown in Fig. 4, compared to the normal form of the *S. eriocheiris* (Fig. 4A), the length of *S. eriocheiris* increased significantly after treatment with Phalloidin (Fig. 4B), while the morphology of *S. eriocheiris* changed from a typical helix to a nearly spherical shape after treatment with A22 (Fig. 4C). The above results suggest that MreB promoter Phalloidin and inhibitor A22 can change the length of *S. eriocheiris* by promoting or inhibiting MreB polymerization. Phalloidin and A22 can change the morphology of *S. eriocheiris* by affecting the polymerization of MreB. To further explore the alteration of *S. eriocheiris* MreB expression at the protein level after treatment with Phalloidin and A22, the *S. eriocheiris* treated with Phalloidin and A22 was broken, and the protein was quantitatively analyzed by MreB specific antibody. There was no significant alteration in the expression of MreB3 and MreB5 after treatment with MreB promoter Phalloidin and MreB inhibitor A22 (Fig. 4D and F). There was no significant difference between MreB4 in Phalloidin treated *S. eriocheiris* and normal *S. eriocheiris*, but the expression of MreB4 was significantly decreased after treatment with A22 (Fig. 4E). The above results suggest that A22 can reduce the expression of MreB and change the morphology of *S. eriocheiris.*

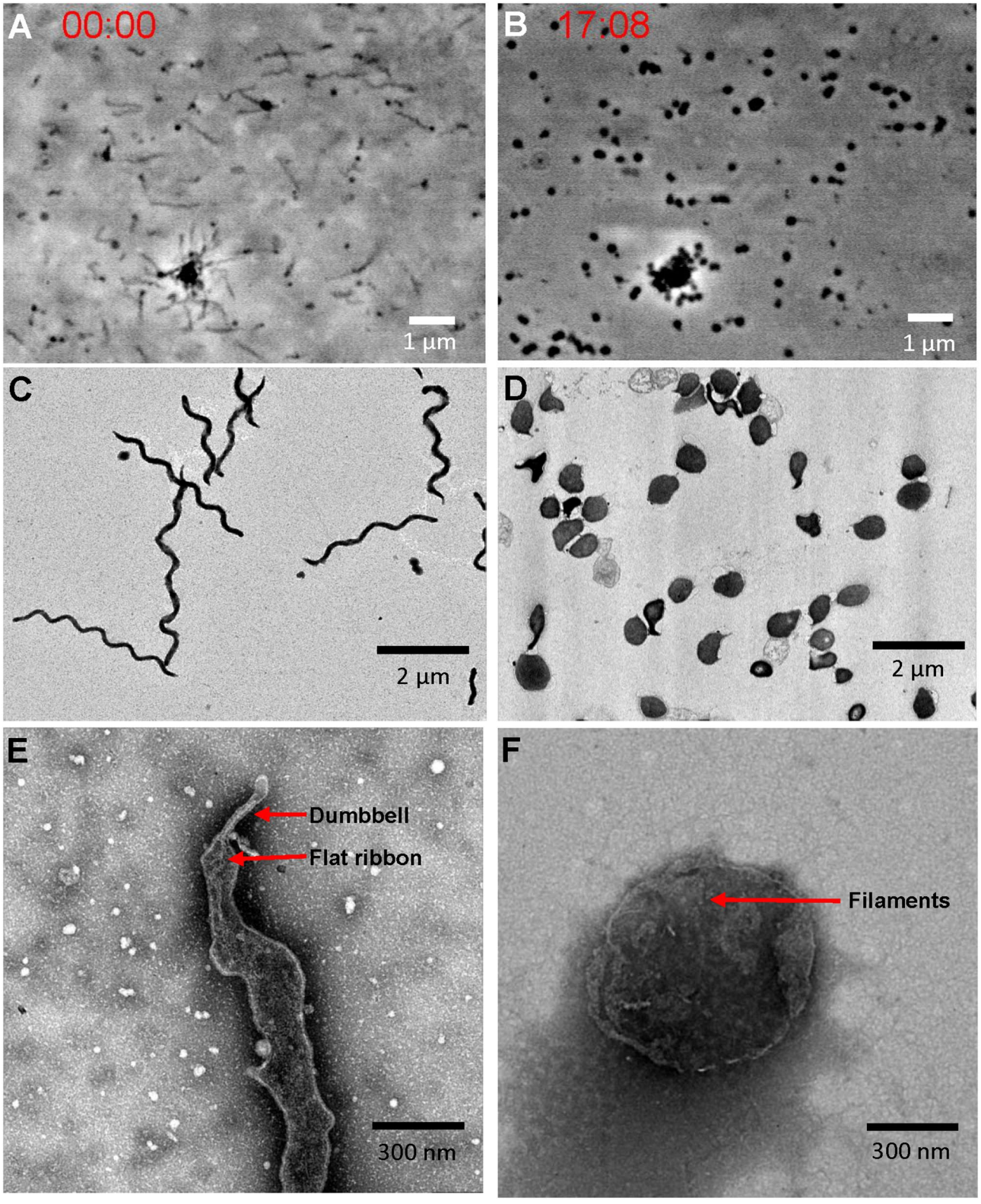

Fig. 1 Morphology of *S. eriocheiris* and cytoskeleton in buffer and H_2O. (**A**) Phase contrast microscope image of *S. eriocheiris* in PBS. *S. eriocheiris* in PBS buffer presents a helical shape. (**B**) Phase contrast microscope image of *S. eriocheiris* in H_2O, where the *S. eriocheiris* appears spherical. (**C**) Negative electron microscopy image of *S. eriocheiris* in PBS, *S. eriocheiris* in PBS is helical shape. (**D**) Electron microscope negative staining image of *S. eriocheiris* in H_2O, the *S. eriocheiris* in H_2O appears spherical. (**E**) The cytoskeleton of *S. eriocheiris* in PBS was observed by electron microscopy. The cytoskeleton of *S. eriocheiris* in PBS showed a slender helical shape. (**F**) The cytoskeleton of *S. eriocheiris* in H_2O was observed under electron microscope, and the cytoskeleton of spherical *S. eriocheiris* in H_2O showed a rounded shape

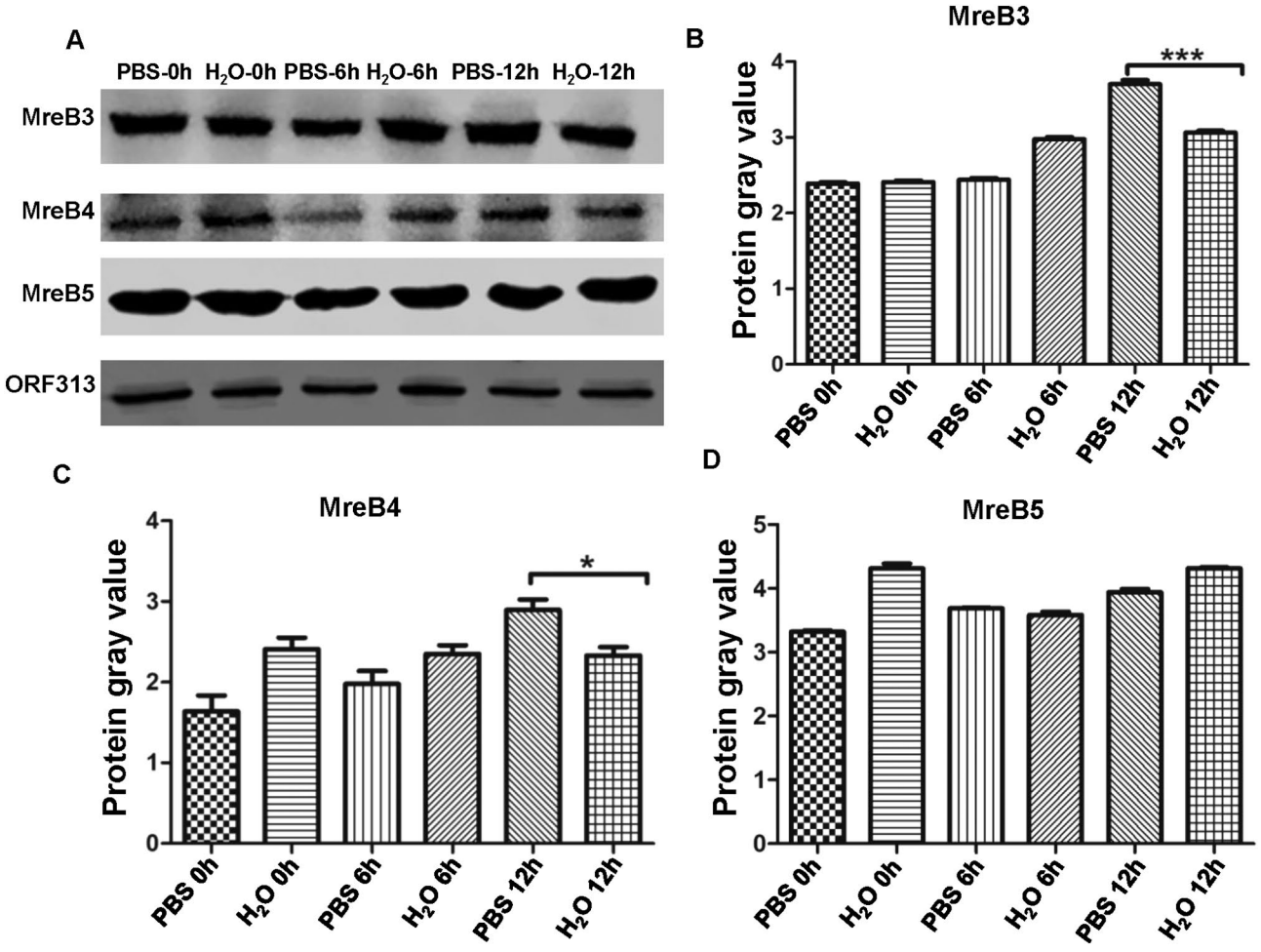

Fig. 2 Alteration of cytoskeleton expression in *S. eriocheiris*. (**A**) Western Blot analysis revealed that *S. eriocheiris* MreB5 in the PBS group did not differ at 0, 6 and 12 h compared to H_2O group, and the expression of MreB3 and MreB4 was also not different at 0 and 6 h, but was higher at 12 h than H_2O group. ORF313 as the internal parameter. (**B**, **C**, **D**) The gray value analysis of Western Blot result of MreB3, MreB4 and MreB5. (*: $p < 0.05$, ***: $p < 0.001$)

Effects of Phalloidin and A22 on the growth of *S. eriocheiris*

To investigate the effect of MreB on the pathogenicity of *S. eriocheiris*, we compared the growth of *S. eriocheiris* under different treatments. After *S. eriocheiris* was treated with 2.5 μg/mL Phalloidin for 12 h, the color of the medium changed from red to yellow, while the color of culture medium only changed slightly after treatment with 200 μg/mL A22 for 12 h (Fig. 5A). The above results showed that the Phalloidin had no significant effect on the growth rate of *S. eriocheiris*, while A22 significantly delayed the growth of *S. eriocheiris*. In order to further explore the effect of Phalloidin and A22 on the number of *S. eriocheiris*, *S. eriocheiris* was treated with 2.5 μg/mL Phalloidin and 200 μg/mL A22, and the number of *S. eriocheiris* was detected by the CCU method. The results showed that compared with the control group, the number of *S. eriocheiris* did not change after treatment with Phalloidin, but decreased to10^6 after treatment with A22 for 12 h (Fig. 5B). The *S. eriocheiris* after treated with A22 was cultured for 8 days, the number of *S. eriocheiris* was as high as 10^8 in the control group (Fig. 5C). These results showed that there was no change in the growth rate and quantity of *S. eriocheiris*, but A22 could significantly slow down the growth rate of *S. eriocheiris*, and had no significant effect on the final number of *S. eriocheiris.*

Effects of Phalloidin and A22 on the mortality of *S. eriocheiris*

To explore whether *S. eriocheiris* could be broken and killed by Phalloidin and A22, *S. eriocheiris* was treated with 2.5 μg/mL Phalloidin and 200 μg/mL A22, and the fragmentation and death of *S. eriocheiris* were detected by flow cytometry. The flow cytometry results showed that compared with the control group (Fig. 6A), there was no significant fragmentation or death of *S. eriocheiris* in the Phalloidin treatment group (Fig. 6B), but 49.5% of the *S. eriocheiris* in the treatment group of A22 showed fragmentation and death (Fig. 6C). The results show that A22 has a certain effect on the fragmentation and death of *S. eriocheiris*. After centrifugation, the *S. eriocheiris* were

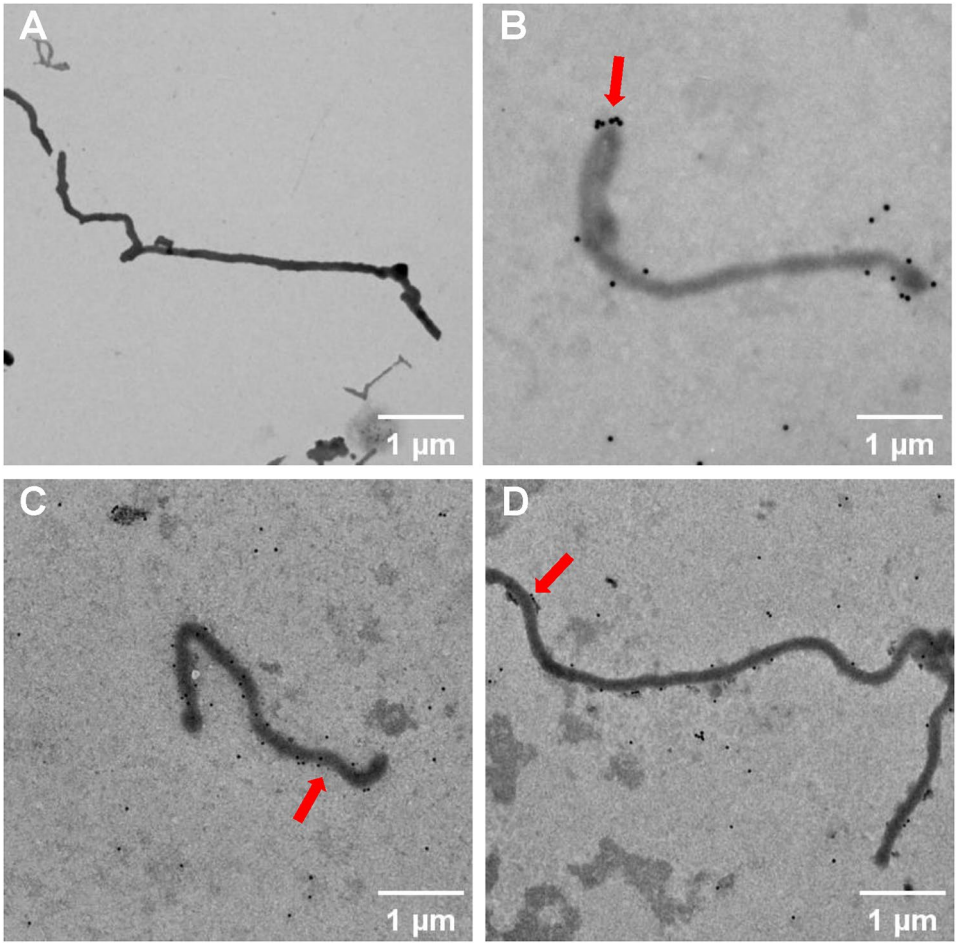

Fig. 3 Localization of MreB in *S. eriocheiris*. (**A**) Immuno-electron microscopy images. No gold particles were observed on the surface of *S. eriocheiris* after incubation with His-tagged protein primary antibody as a negative control. (**B**, **C**) Immuno-electron microscopy image. The *S. eriocheiris* was incubated with a primary antibody specific to MreB3 and MreB4, and gold particles were observed in an aggregated state at one end of the organism, as indicated by the red arrow. (**D**) Immuno-electron microscopy images. The strain was incubated with a primary antibody specific to MreB5, resulting in the even distribution of gold particles on the surface of *S. eriocheiris*, as indicated by the red arrow

resuspended with R2, and each *E. sinensis* was injected with 100 μL *S. eriocheiris*, and the number of deaths was counted every day. The result revealed a diminished *E. sinensis* survival rate in the Phalloidin group compared to the untreated, wild-type *S. eriocheiris* group at 5, 7, and 9 days post-infection (Fig. 6D), suggesting that Phalloidin may amplify the pathogenicity of *S. eriocheiris*. Conversely, the A22 treated group displayed an elevated *E. sinensis* survival rate relative to the untreated wild-type *S. eriocheiris* group at 7 and 9 days (Fig. 6D), indicating a potential reduction in *S. eriocheiris* pathogenicity due to A22. Notably, no significant difference in *E. sinensis* survival rates was observed between the wild-type *S. eriocheiris* group, the A22 treated group, and the Phalloidin treated group 9 days following the injection.

Effects of *S. eriocheiris* treated with Phalloidin and A22 on blood lymphocytes

Morphology of blood lymphocytes

To explore the effect of *S. eriocheiris* treated with Phalloidin and A22 on blood lymphocytes of *E. sinensis*, *S. eriocheiris* treated with 2.5 μg/mL Phalloidin and 200 μg/mL A22 were used to infect blood lymphocytes of *E. sinensis*. Blood lymphocytes were observed by inverted fluorescence microscope at 0, 12 and 24 h after infection. It was found that the blood lymphocytes were basically normal fusiform or ellipsoidal type at 0 h (Fig. 7A). Compared with negative control group, *S. eriocheiris* treated with Phalloidin and A22 group, and *S. eriocheiris* in the positive control group infected blood lymphocytes for 12 h, a small number of cell fragments were found in all three groups, but the morphology of blood lymphocytes basically remained normal (Fig. 7B). After 24 h of infection, most of the blood lymphocytes in the Phalloidin group were granular, the number of cells decreased

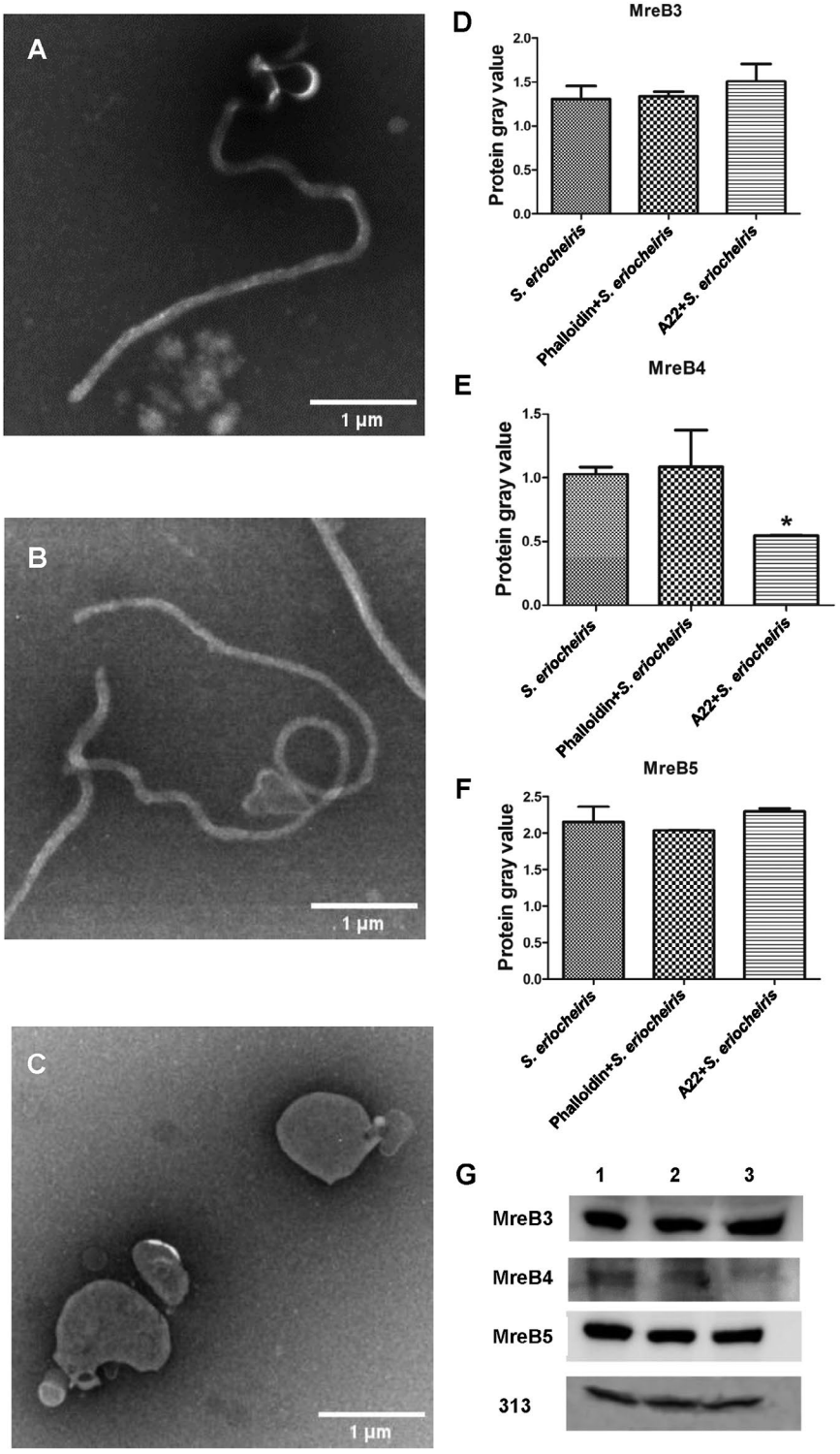

Fig. 4 Morphology of *S. eriocheiris* and expression of the cytoskeleton protein MreB after treatment with Phalloidin and A22. (**A**, **B**, **C**) *S. eriocheiris*'s TEM negative staining images. **A**, using *S. eriocheiris* as a negative control. **B**, the length of *S. eriocheiris* was significantly increased after treatment with Phalloidin. **C**, the morphology of *S. eriocheiris* transformed from a spiral shape to an almost spherical shape following treatment with A22. (**D**, **E**, **F**) The gray value of MreB3, MreB4 and MreB5 in *S. eriocheiris*, following treatment with Phalloidin and A22, **D** and **F** did not exhibit significant alterations in expression levels. **E**, the expression of MreB5 was significantly reduced after A22 treatment of *S. eriocheiris*. (**G**) Western blot analysis of the expression of the skeleton protein MreB, SPE-0313 was used as reference. 1: *S. eriocheiris* without any treatment as control. 2: MreB expression in *S. eriocheiris* after treatment with Phalloidin. 3: MreB expression in *S. eriocheiris* after treatment with A22. (*: $p < 0.05$)

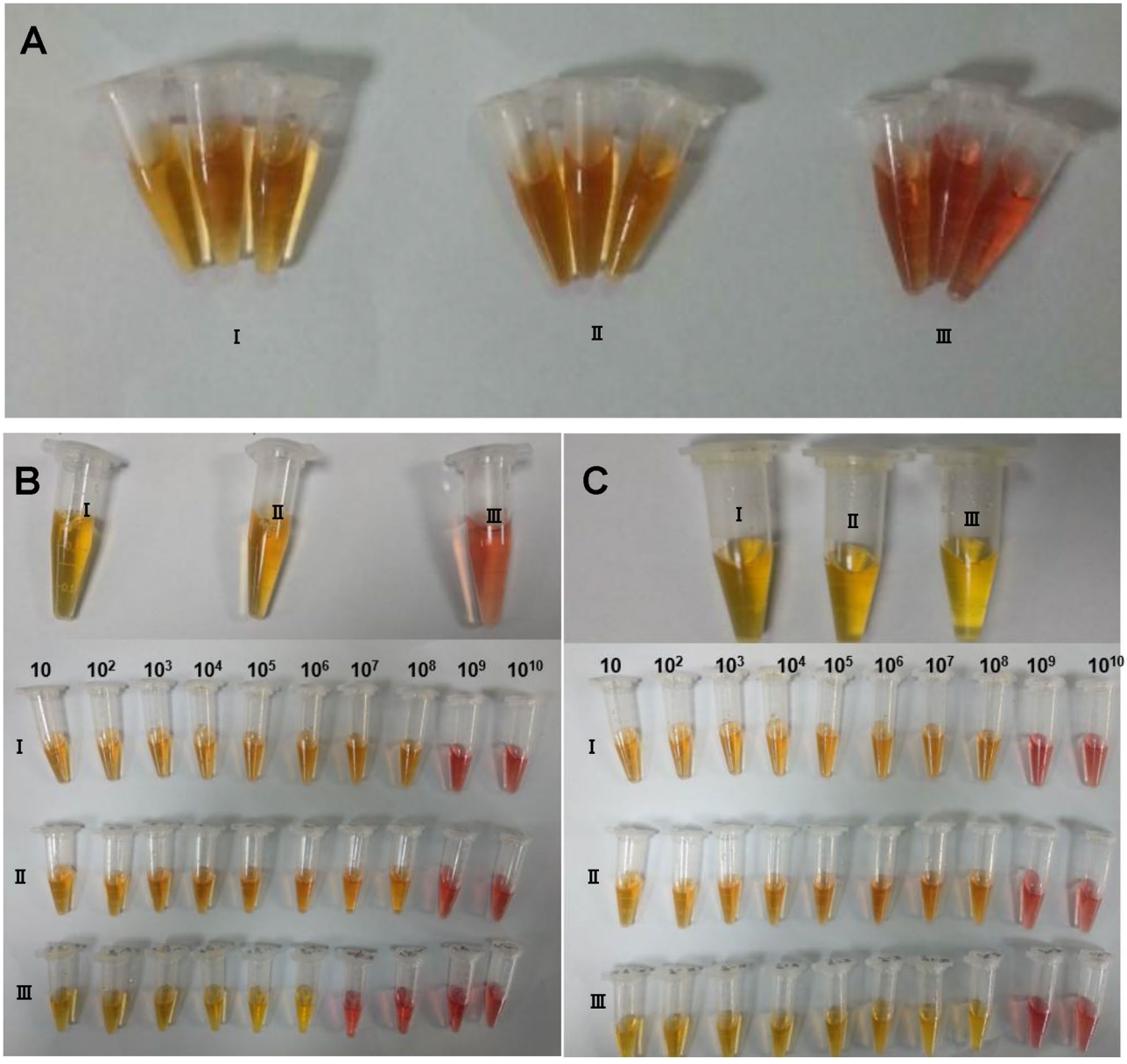

Fig. 5 The impact of Phalloidin and A22 on the *S. eriocheiris* growth. (**A**) The alterations of the medium color of *S. eriocheiris* after treatment with Phalloidin and A22. I: *S. eriocheiris* as negative control. II: *S. eriocheiris* was treated with 2.5 μg/mL Phalloidin for 12 h, the medium color changed from red to yellow. III: *S. eriocheiris* after treatment with 200 μg/mL A22 for 12 h, the medium color slightly changed. (**B**) Calculating the number alterations of *S. eriocheiris* in the first three groups presented in **5A** using CCU method. I: In the negative control group, the number of *S. eriocheiris* can reach 10^8. II: The number of *S. eriocheiris* treated with Phalloidin could also reach 10^8, without alterations. III: The number of *S. eriocheiris* was reduced after 12 h treatment with A22, and only reached 10^6. (**C**) The front of three groups of *S. eriocheiris* were cultivated for 8 days, and calculated the alterations of number by CCU method. I: Negative control group. II: The number of *S. eriocheiris* could also reach 10^8 after treatment with Phalloidin, without alterations. III: The number of *S. eriocheiris* treated with A22 could also reach 10^8 after culture for 8 days

significantly, many cells were broken and died, and the cells were surrounded by contents and impurities. However, the survival rate of blood lymphocytes in the A22 treatment group was higher than that in the positive control group, and the membrane growth halo of the surviving cells was obvious, which maintained the normal growth state (Fig. 7C). The above results showed that *S. eriocheiris* treated with Phalloidin worsened the morphology of blood lymphocytes of *E. sinensis*, while *S. eriocheiris* of A22 group had less effect on the morphology of *E. sinensis* blood lymphocytes.

The ability of S. eriocheiris to invade blood lymphocytes

Compared with the positive control group, the cell morphology of the Phalloidin treatment group was slightly worse, while the A22 treatment group was slightly

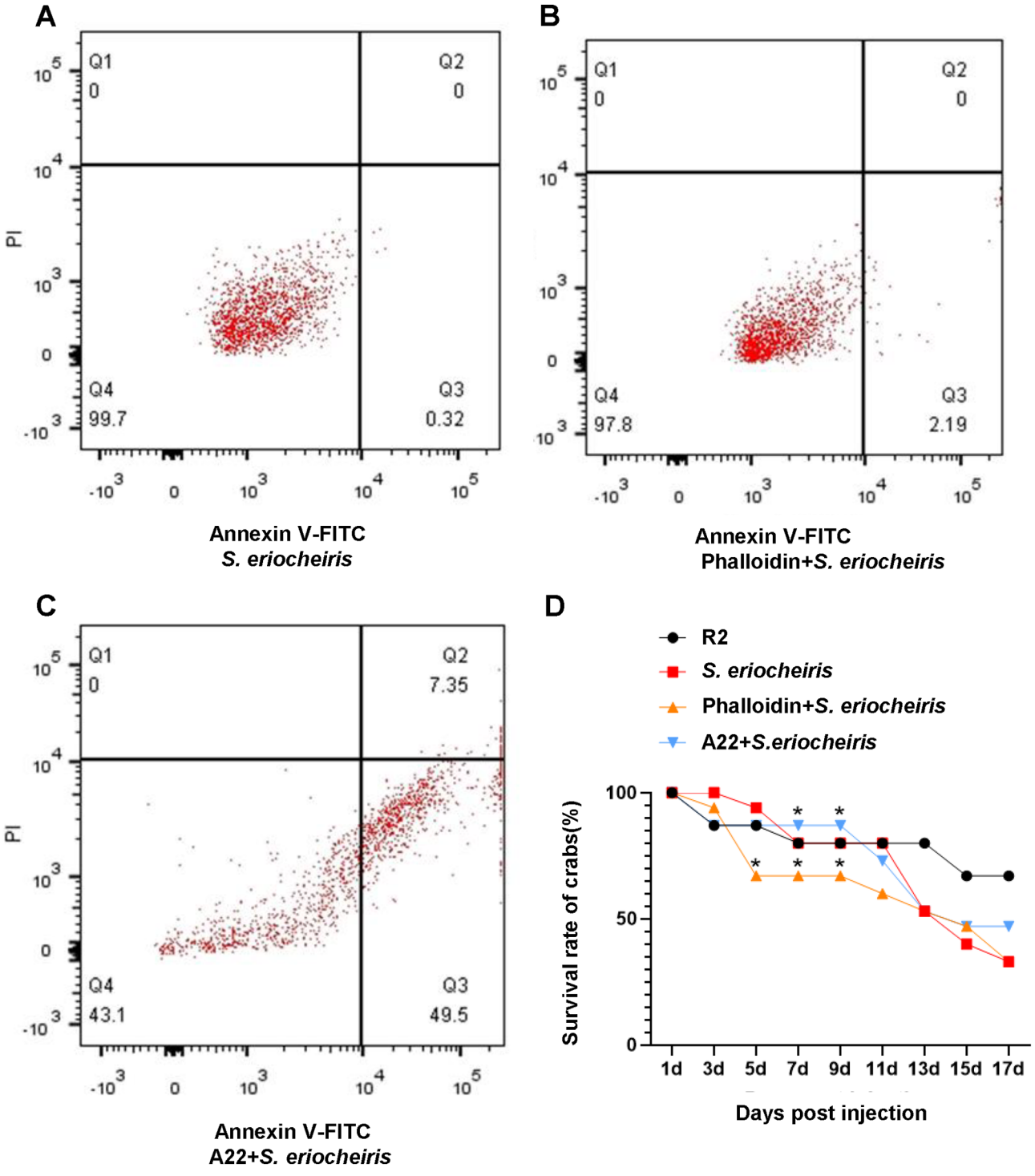

Fig. 6 Effects of Phalloidin and A22 on mortality and virulence of *S. eriocheiris*. (**A**) The death of *S. eriocheiris* was detected by flow cytometry, it is the control group. (**B**) No significant fragmentation and death of *S. eriocheiris* treated with Phalloidin compared to the control group. (**C**) 49.5% of the *S. eriocheiris* in the A22 treatment group were fragmented and dead. (**D**) The survival rate of *E. sinensis* infected with *S. eriocheiris* treated with Phalloidin and A22. The survival rate of *S. eriocheiris* in the Phalloidin group was lower than the *S. eriocheiris* group at 5, 7 and 9 days, the survival rate of A22 treated group was higher than *S. eriocheiris* group at 7, and 9 days. (* indicates a significant difference between this group and the *S. eriocheiris* group)

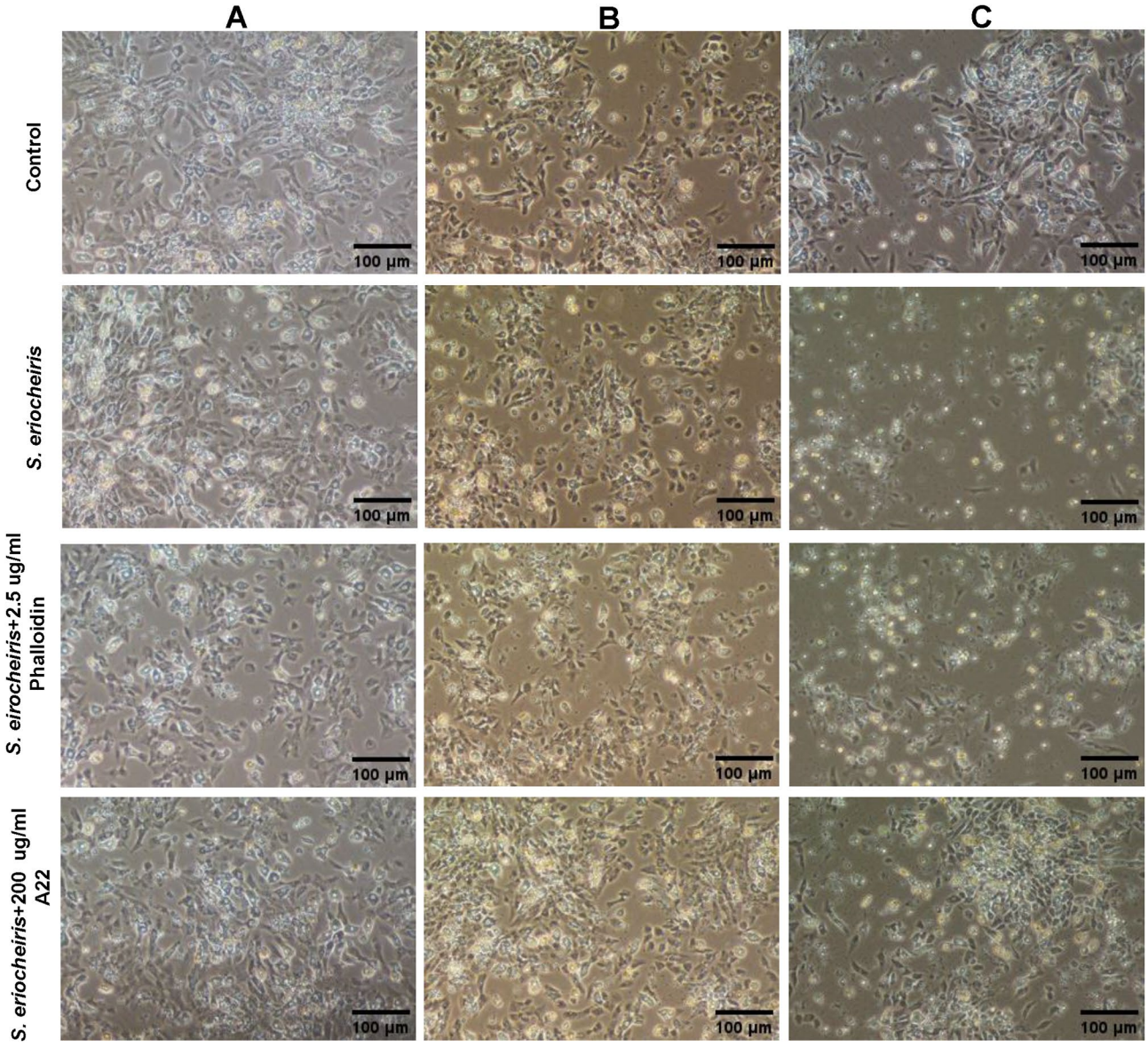

Fig. 7 Blood lymphocytes morphology of *E. sinensis* under phase contrast microscope. (**A**) The column results show that the blood lymphocytes of *E. sinensis* were infected with wild type *S. eriocheiris* and *S. eriocheiris* treated with Phalloidin and A22 after 0 h, the hemolymph cells were basically normal fusiform or ellipsoid shape. (**B**) Compared with the negative control group, the other three groups of *S. eriocheiris* showed a small number of cellular debris after the blood lymphocytes were infected for 12 h, but the morphology of the blood lymphocytes was basically maintained in a normal state. (**C**) After 24 h of infection, the number of blood lymphocytes in the Phalloidin group was significantly reduced. Compared with the positive control group, the survival rate of blood lymphocytes in the A22-treated group was increased, and the surviving cells maintained the morphology of the normal growth state

better. To further verify this phenomenon, we detected the effects of *S. eriocheiris* infection treated with Phalloidin and A22 on the viability of blood lymphocytes using Cell Counting Kit-8. As shown in Fig. 8, taking the cell viability of the negative control group as the standard, 12 and 24 h after *S. eriocheiris* infection, the cell activity in the Phalloidin group was significantly lower than that in the positive control group (Fig. 8A). However, the cell activity in A22 treatment group was significantly increased (Fig. 8B). The results showed that the infection of *S. eriocheiris* to blood lymphocytes was enhanced and the cell viability was significantly decreased in Phalloidin treatment group, while the infection of blood lymphocytes by *S. eriocheiris* in A22 group was significantly decreased and the cell viability was significantly increased. To investigate whether the changes of cell viability and morphology are directly related to *S. eriocheiris* infection, we detected the copies of *S. eriocheiris* in the blood lymphocytes of the Phalloidin group (*S. eriocheiris*+2.5 μg/ml Phalloidin), A22 group (*S. eriocheiris*+200 μg/ml A22) and positive control group (*S. eriocheiris*). It was found that there was no significant

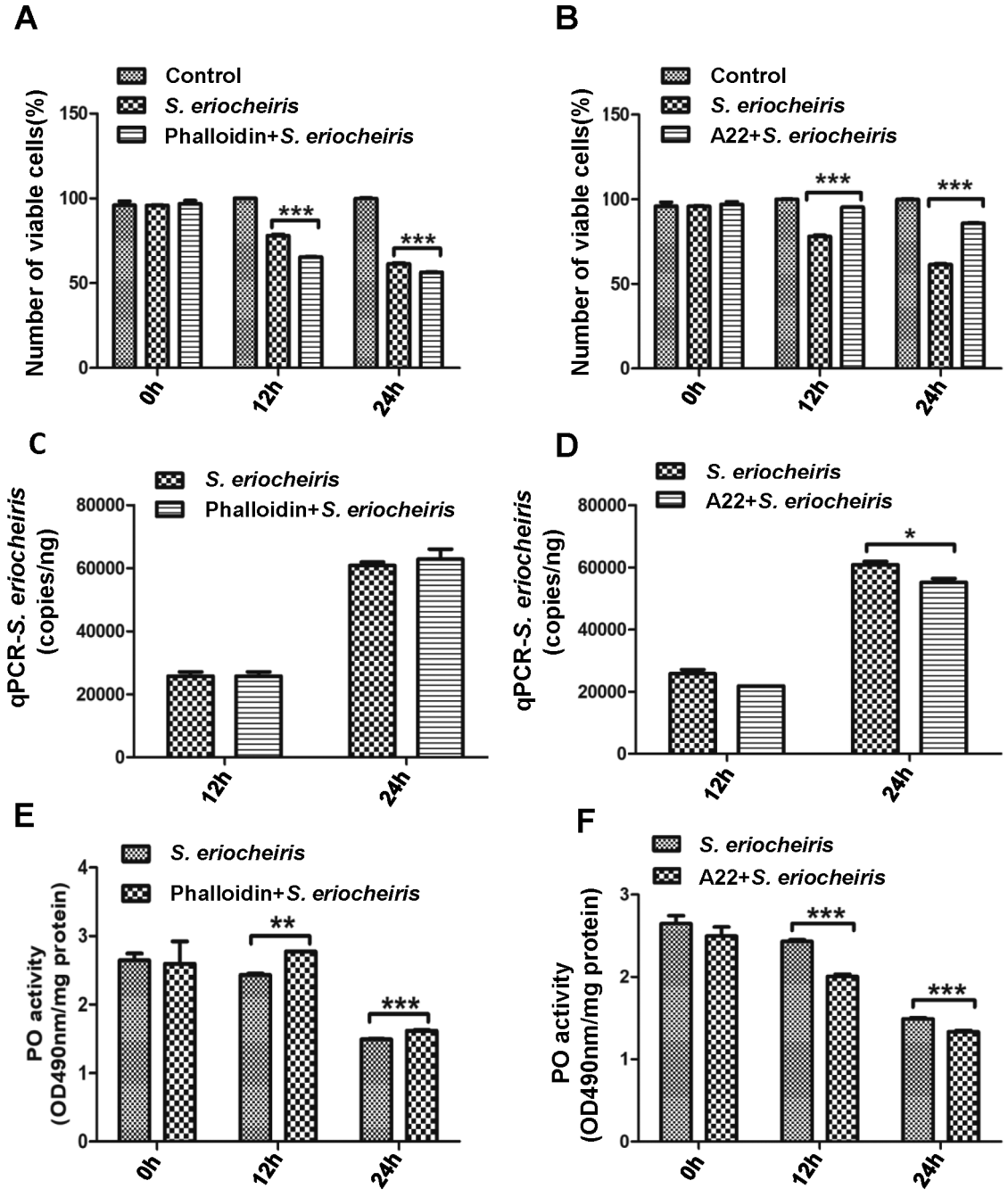

Fig. 8 Effects of *S. eriocheiris* on *E. sinensis* blood lymphocytes. (**A**, **B**) Activity of blood lymphocytes infected with *S. eriocheiris* and *S. eriocheiris* treated with Phalloidin and A22. Using the negative control group as the standard, the cell viability of the Phalloidin group was significantly lower than the positive control group after 12 and 24 h of *S. eriocheiris* infection, while the cell viability of the A22 group was significantly higher (***: $p < 0.001$). (**C**, **D**) When *S. eriocheiris* was treated with Phalloidin, the intracellular *S. eriocheiris* copy number did not change significantly at 12 and 24 h after infection compared with the control group. The copy number of A22 group did not change significantly at 12 h, but it was significantly lower than the normal group at 24 h. (*: $p < 0.05$). (**E**, **F**) When *E. sinensis* was infected with *S. eriocheiris* of the Phalloidin group, the PO activity of blood lymphocytes was significantly higher after 12 h and 24 h compared with the positive control group, while the PO activity of blood lymphocytes in the A22-treated group was significantly lower than that in the positive control group. (***: $p < 0.001$, **: $p < 0.01$)

change in the copy number of *S. eriocheiris* in the Phalloidin treatment group compared with the control group at 12 and 24 h after infection (Fig. 8C), while there was no significant change in the copy number of *S. eriocheiris* infected blood lymphocytes in the A22 group after 12 h, but it was significantly lower than that in the positive control group after 24 h (Fig. 8D). This result showed that the ability of *S. eriocheiris* treated with A22 to infect

blood lymphocytes and replicate in them was decreased. To explore the changes of phenoloxidase system of blood lymphocytes induced by *S. eriocheiris* treated with Phalloidin and A22, blood lymphocytes were infected with *S. eriocheiris* treated with Phalloidin and A22, and the activity of PO was detected. PO is an innate immune protein whose increase in blood lymphocytes helps to resist infection by pathogens. The results showed that compared with the positive control group, the activity of PO increased significantly 12 and 24 h after Phalloidin group infection (Fig. 8E). After 12 and 24 h of *S. eriocheiris* infection, the activity of PO in the A22 treatment group was significantly lower than that in the positive control group (Fig. 8F). The above results show that infection of *S. eriocheiris* treated with both Phalloidin and A22 can affect the PO activity of blood lymphocytes. PO is a kind of innate immune protein, and its elevation in blood lymphocytes is helpful to resist the infection of pathogens. Because the PO activity of blood lymphocytes infected by *S. eriocheiris* treated with A22 was significantly lower than that of the positive control group, which indicated that the pathogenicity of *S. eriocheiris* treated with A22 was weakened.

Apoptosis of blood lymphocytes infected by S. eriocheiris

To further explore the effects of *S. eriocheiris* treated with Phalloidin and A22 on the apoptosis and necrosis of blood lymphocytes, blood lymphocytes infected with *S. eriocheiris* were collected to detect apoptosis. The flow cytometry results showed that after 24 h of normal *S. eriocheiris* infection, 17.6% of the cells were necrotic, 77.3% of the cells had late withering, and 3.61% of the cells had early withering (Fig. 9A). After 24 h of *S. eriocheiris* infection treated with Phalloidin, 22.3% of the cells were necrotic, 72.0% of the cells were late withered, and 3.01% of the cells were withered early (Fig. 9B). After 24 h of the blood lymphocytes of the A22 group infected with *S. eriocheiris*, only 11.6% of the cells were necrotic, but 82.0% of the cells had late apoptosis and 3.85% of the cells had early apoptosis (Fig. 9C). The above results showed that the number of cell necrosis of blood lymphocytes infected with Phalloidin group increased, while the number of necrotic A22-treated cells decreased.

Discussion

The role of MreB in the morphology of *S. eriocheiris*

In recent years, the research on the cytoskeleton of *Spiroplasma* mainly focuses on the *Spiroplasma*-specific fibril proteins, while the actin-like protein MreB has been less frequently reported. Studies on the *Spiroplasma* cytoskeleton have also only modeled its distribution in the cytoskeletal structure mathematically and physically, and studies on its biological function are lacking [22]. We focused on MreB to explore its biological function in the cytoskeleton structure, and to understand its role in morphological changes. Because *S. eriocheiris* has no cell wall, its morphology is variable, and *S. eriocheiris* has different morphology at different growth stages, it has a more typical helical structure during the logarithmic growth phase, and helix during the plateau phase when nutrient conditions are adequate, but takes on several different morphologies during the nutrient-deficient plateau phase and the decay phase, such as dumbbell-shaped, bean-shaped, spherical, pear-shaped, and tadpole-shaped and other irregular shapes. These morphological variations are closely related to the cytoskeleton. *S. eriocheiris* is typical helix shape during logarithmic growth and spherical during decay, and the transcripts of all five

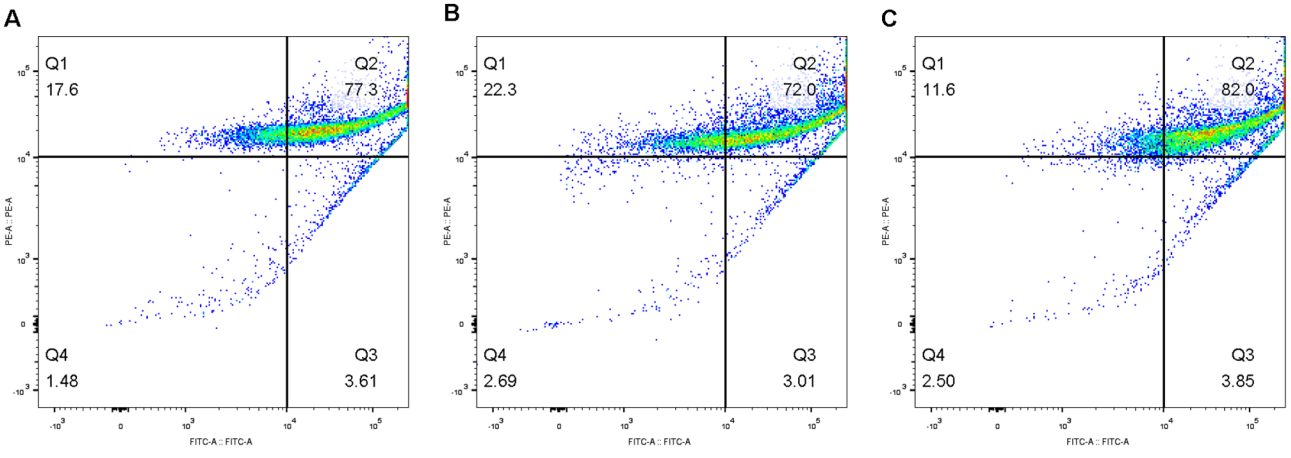

Fig. 9 Flow cytometry detection of blood lymphocytes apoptosis infected with *S. eriocheiris* treated with Phalloidin and A22. (**A**) The flow cytometry results showed that blood lymphocytes was infected with normal *S. eriocheiris,* necrosis occurred in 17.6% of the cells, late apoptosis in 77.3% and early apoptosis in 3.61% of the cells after 24 h. (**B**) After 24 h infection of blood lymphocytes with *S. eriocheiris* treated with Phalloidin, necrosis occurred in 22.3% of the cells, late apoptosis in 72.0%, and early apoptosis in 3.01% of the cells. (**C**) Blood lymphocytes was infected with *S. eriocheiris* treated with A22, necrosis occurred in 11.6% of the cells, late apoptosis in 82.0%, and early apoptosis in 3.85% of the cells after 24 h

MreB genes are significantly different between the two phenotypes (unpublished data). The morphology of *S. melliferum* was observed by dark field microscope, and it was found that most of the *S. melliferum* bodies were dots in the early stage of hysteresis. Electron microscopy revealed that they were mainly irregular near-spherical or slightly curved rod-shaped with swollen ends, while the morphology of *S. eriocheiris* in the logarithmic growth phase was mainly typical helical. It was also found that there were significant differences in the transcription of MreB5 gene between helical and non-helical *S. melliferum*, and the transcription amount of MreB gene in helical was significantly higher than that in non-helical [32]. In the *S. poulsonii*, the MreB subtype forms a polymeric cytoskeleton that acts on the bacteria morphology in a wall-independent manner, however, the high expression of MreB3 is not sufficient to form the bacteria helicity which needs to interact with MreB5 to perform function, the MreB polymeric structures coordinate fibril cytoskeleton, and membrane to maintain the helicity of *Spiroplasma*, and in in wall-less bacteria, they control the shape of the bacteria through mechanisms independent of peptidoglycan synthesis [19, 33]. The maintenance of helical morphology of *Spiroplasma* is also closely related to its motility mechanism. Fibril is a constitutive filament-forming cytoskeletal protein that makes up filaments and is unique to members of the genus *Spiroplasma* [34].The five homologues of MreB interact with each other and form the ribbon structure of the *Spiroplasma* with the fibril, the cell rotates its body by transmitting helicity and switching along the cell axis, thus moving forward. The helicity transition and its transmission may be caused by conformational changes in the internal helical band structure along the entire cell axis [35, 36]. The combination of *S. eriocheiris* MreB4-MreB5 and MreB1-MreB5 produces the helical morphology and swimming ability, but the reason for the presence of up to five MreBs is not known, in different environments, they may favour efficient and robust swimming. Some studies have shown that when MreB is combined with filaments, MreB exerts a force on the filaments while swimming, and the filaments may also effectively obtain high energy efficiency and chemotaxis [12, 18].

Similarly, the role of MreB on *Spiroplasma* morphology and motility has been demonstrated in *S. citri*. In the nonhelical strain *S. citri ASP-1*, the loss of helicity and motility is due to a nonsense mutation within the sequence encoding MreB5 that cannot be functionally compensated by any of the other four MreBs. Thus, MreB5 was identified as a major determinant of cell helicity in *S. citri* [37]. In addition, the researchers found a lipoprotein on the locus encoding MreB in *S. citri*, which does not interact functionally with MreB, but may positively affect the survival of Citri clade by swimming [38]. A22 is an antibiotic-like small molecule compound that prevents the assembly of MreB and specifically binds to sites on MreB [39]. Our experiment showed that the *S. eriocheiris* was approximately spherical after A22 treatment, and the expression level of MreB4 was significantly decreased at this time, which suggested that the deformation effect of A22 on *S. eriocheiris* may mainly depend on MreB4. In summary, MreB plays an important role in the morphology alteration of *S. eriocheiris.*

The role of cytoskeleton proteins MreB in the pathogenesis of *S. eriocheiris*

The invasion of *S. eriocheiris* into *E. sinensis* has caused great losses to the aquaculture industry, and studies have shown that *S. eriocheiris* has been observed in blood lymphocytes as well as in other organs of the *E. sinensis*, making it clear that blood lymphocytes are the target cells of *S. eriocheiris* [40]. We used *S. eriocheiris* treated with MreB promoter Phalloidin and inhibitor A22 to infect the blood lymphocytes of *E. sinensis*, the ability of *S. eriocheiris* to destroy blood lymphocytes was significantly weakened after A22 treatment, and the cell activity was significantly increased compared with the *S. eriocheiris* control group, the flow cytometry results also showed that the amount of cell necrosis was lower than *S. eriocheiris* control group. Compared with the control group, the destructive ability of *S. eriocheiris* treated with Phalloidin was enhanced and the cell viability was significantly reduced. Flow cytometry results showed an increase in cell necrosis as well. It has been shown that Drosophila S2 cells infested with *S. eriocheiri* exhibit cytopathic effects, mainly in the form of a gradual deterioration in the state of the cells. The formerly well adherent cells gradually shrink and become surrounded by exudate or cellular debris. Meanwhile, *S. eriocheiris* induces apoptosis in S2 cells, and the viability of S2 cells severely decreases with the prolongation of infection [41]. The viability of 3T6 cells was also decreased after *S. eriocheiris* infection of mouse 3T6 cells [42]. In addition, *S. eriocheiris* infected the blood lymphocytes of *E. sinensis*, and the cytopathic effect occurred within 36 h, with the morphology changing from initially radial to irregular mass [43]. In the present study, we found that *S. eriocheiris* treated with Phalloidin was able to infect blood lymphocytes, destroy the morphology of the cells, significantly reduce cell viability, and induce apoptosis, which is strongly pathogenic. Phalloidin is a polypeptide isolated from mushroom *Amanita phalloides* [44]. In eukaryotes, Phalloidin mainly causes hepatocyte necrosis [45–47], Phalloidin binds to F-actin, stabilizes F-actin filaments, and irreversibly prevents filamentous F-actin from depolymerizing into globular G-actin, the bile ducts are wrapped in actin filaments, reducing bile flow and leading to cholestasis [29]. Since the MreB protein in *S.*

eriocheiris is homologous to eukaryotic actin [15], the Phalloidin may have a stable function on MreB, but did not increase the MreB expression. Previous studies have shown that MreB is associated with the ability of *S. eriocheiris* to swim [17], the effect of Phalloidin on MreB may allow it to maintain a good motility and thus enhance its pathogenicity, however, due to the differences between eukaryotes and prokaryotes, it is necessary to further explore whether Phalloidin have different pathogenic targets for *S. eriocheiris*.

MreB is one of the cytoskeleton proteins of *S. eriocheiris* and has an important role in maintaining the morphology of *S. eriocheiris* [13]. It has also been found that MreB is a virulence gene for pathogenic bacteria [48]. A study on the cytoskeleton proteins of *Salmonella* revealed a strong link between the cytoskeleton and pathogenicity, and the expression of virulence genes was directly related to the integrity of the cytoskeleton [49]. *E263* bacteria expressing MreB-GFP were treated with A22 for 30 min and then infected with purified *GVE2* virus, it was found that A22 could change the bacteria morphology by blocking the polymerization of MreB in the host bacteria, and the blocking of MreB polymerization directly inhibited the infection of *GVE2* to the host bacteria [50]. *Shigella* is a gram-negative rod-shaped bacterium, one of the pathogens of bacillary dysentery, its rod-shaped structure is necessary for invading host cells, and its growth is not inhibited by A22. There was no significant difference in the cell adhesion capacity of *Shigella* with a spherical shape after A22 induction, but the cell invasion rate of *Shigella* rapidly decreased when the concentration of A22 was 5 mg/mL [51], indicating that the cell invasion of *Shigella* MreB was inhibited after the morphology change caused by the A22 obstruction. These experimental results showed that when the polymerization of MreB was inhibited by A22, the pathogenicity of bacteria was also affected, indicating that MreB also plays an important role in the pathogenicity of bacteria. The administration of A22 to *S. eriocheiris* yielded a notable increase in *E. sinensis* mortality rates 7 and 9 days post-infection (Fig. 6D). Conversely, the Phalloidin group exhibited decreased mortality at 5, 7, and 9 days relative to the untreated, wild-type *S. eriocheiris* group (Fig. 6D). These findings suggest that MreB significantly influences the pathogenicity of *S. eriocheiris*. Notably, no statistically significant difference in *E. sinensis* survival rates was observed between the wild-type *S. eriocheiris* group, the A22 treated group, and the Phalloidin treated group after 9 days post-injection. This may be attributed to the specific action of A22 and Phalloidin on MreB protein, as neither agent affects the MreB gene. Consequently, newly formed *S. eriocheiris* daughter cells possess the structure and function of native MreB, resulting in a pathogenesis comparable to the wild-type *S. eriocheiris*. Similarly, the growth of *S. eriocheiris* after treatment with A22 confirmed this explanation. Studies suggested that MreB also plays a crucial role in bacterial division [52], *S. eriocheiris* treated with A22 had a delayed growth due to the inhibition of MreB, which affected their ability to divide, however, A22 did not affect the MreB gene, *S. eriocheiris* can grow normally after prolonged the cultivation time. MreB has various functions in *S. eriocheiris*, which can affect its morphology and swimming ability [16, 53], therefore, inhibition of MreB by A22 leads to the decrease of *S. eriocheiris* pathogenicity. In addition, after the infection of *S. eriocheiris* treated with A22 in blood lymphocytes, there were still a small number of blood lymphocytes with normal morphology, and the cell viability was also significantly increased compared with normal *S. eriocheiris*. Our work illustrates that the pathogenicity of *S. eriocheiris* was significantly reduced in the presence of the cytoskeletal MreB inhibitor A22, which suggests that MreB has an important role in *S. eriocheiris* pathogenicity.

Conclusion

In contrast to other members of the wall-less *Mollicutes* family, the *S. eriocheiris* genome has retained the MreB gene throughout evolution [16]. In this study, we successfully prepared three MreB recombinant proteins and elucidated the role of this protein in the cytoskeleton of *S. eriocheiris* as well as its effect on the pathogen's virulence. Following treatment with the cytoskeletal protein promoter Phalloidin and the cytoskeletal protein inhibitor A22, the length of *S. eriocheiris* in the treatment group was significantly longer compared to the control group. Conversely, the length of *S. eriocheiris* in the A22 treatment group was significantly reduced, resulting in nearly spherical cells. Western Blot analysis revealed that after treatment with phalloidin and A22 showed no significant changes in the expression levels of MreB3, MreB4, and MreB5 in the Phalloidin-treated group. However, there was a notable decrease in the expression of MreB4 in the A22-treated group, while the expression of MreB3 and MreB5 remained comparable to the levels in normal *S. eriocheiris*. Furthermore, observations of the growth status of *S. eriocheiris* and the characteristics of its blood lymphocytes indicated that the pathogenicity of *S. eriocheiris* was significantly altered by cytoskeletal MreB stabilizator and inhibitor. Specifically, the pathogenicity of *S. eriocheiris* treated with Phalloidin was significantly enhanced, whereas it was markedly reduced when treated with the inhibitor A22. Our findings suggest that the MreB protein in *S. eriocheiris* plays a crucial role in its morphology and pathogenicity, providing new insights into potential strategies for the prevention and control of *S. eriocheiris* infections.

Supplementary Information

The online version contains supplementary material available at https://doi.org/10.1186/s13062-024-00537-3.

Supplementary Material 1

Acknowledgements
None.

Author contributions
Conception and design were done by Rong Li, Xiaohui Cao, Jiaxin Chen, Tingting He and Wen Wang (MreB purification and morphology parts), Yan Zhang, Siyuan Zhang, Yaqi Wang and Yifei Wang (Pathogenicity part). Collection and assembly of data were done by Yanyan Qiu, Mengji Xie and Yuhua Xu (MreB purification and morphology parts) and Kailin Shi (Pathogenicity part). Manuscript writing was done by Rong Li and Peng Liu. Final approval of manuscript was done by Peng Liu.

Funding
This work was supported by the National Natural Science Foundation of China (NSFC) [32370209]; Natural Science Foundation of Hunan Province, China [2023JJ30503]; Scientific Research Foundation of Hunan Provincial Education Department, China [22A0297]; and Hunan Provincial College Students' innovation and Entrepreneurship Training Program [S202310555204, S202312650005, X202410555207, S202410555051, X202410555214].

Data availability
No datasets were generated or analysed during the current study.

Declarations

Ethics approval and consent to participate
Not applicable.

Consent for publication
Not applicable.

Competing interests
The authors declare no competing interests.

Received: 18 July 2024 / Accepted: 26 September 2024
Published online: 23 October 2024

References

1. Bi K, Du J, Chen J, Wang H, Zhang K, Wang Y, et al. Screening and functional analysis of three *Spiroplasma eriocheiris* glycosylated protein interactions with *Macrobrachium nipponense* C-type lectins. Fish Shellfish Immunol. 2023;138:108810.
2. Whitcomb RF. The genus *Spiroplasma*. Annu Rev Microbiol. 1980;34:677–709.
3. Clark TB, Henegar RB, Rosen L, Hackett KJ, Whitcomb RF, Lowry JE, et al. New spiroplasmas from insects and flowers: isolation, ecology, and host association. Isr J Med Sci. 1987;23(6):687–90.
4. Hou L, Du J, Ren Q, Zhu L, Zhao X, Kong X, et al. Ubiquitin-modified proteome analysis of *Eriocheir sinensis* hemocytes during *Spiroplasma eriocheiris* infection. Fish Shellfish Immunol. 2022;125:109–19.
5. Ning M, Xiu Y, Yuan M, Bi J, Hou L, Gu W, et al. *Spiroplasma eriocheiris* Invinton Into *Macrobrachium rosenbergii* Hemoistmediateddiated by Patenolaseno-lase and Host Lipopolysaccharide and β-1, 3-Gbindingiproteinrotein. Front Immunol. 2019;10:1852.
6. Wang Y, Miao Y, Shen Q, Liu X, Chen M, Du J, et al. *Eriocheir sinensis* vesicle-associated membrane protein can enhance host cell phagocytosis to resist *Spiroplasma eriocheiris* infection. Fish Shellfish Immunol. 2022;128:582–91.
7. Wang W, Wen B, Gasparich GE, Zhu N, Rong L, Chen J, et al. *A* spiroplasma associated with tremor disease in the Chinese mitten crab (*Eriocheir sinensis*). Microbiol (Reading). 2004;150(Pt 9):3035–40.
8. Regassa LB, Gasparich GE. *Spiroplasmas*: evolutionary relationships and biodiversity. Front Bioscience: J Virtual Libr. 2006;11:2983–3002.
9. Srisala J, Pukmee R, McIntosh R, Choosuk S, Itsathitphaisarn O, Flegel TW, et al. Distinctive histopathology of *Spiroplasma eriocheiris* infection in the giant river prawn *Macrobrachium rosenbergii*. Aquaculture. 2018;493:93–9.
10. Liang T, Li X, Du J, Yao W, Sun G, Dong X, et al. Identification and isolation of a *spiroplasma* pathogen from diseased freshwater prawns, *Macrobrachium rosenbergii*, in China: a new freshwater crustacean host. Aquaculture. 2011;318(1):1–6.
11. Xiu N, Yang C, Chen X, Long J, Qu P. Rare *Spiroplasma* bloodstream infection in patient after surgery, China, 2022. Emerg Infect Dis. 2024;30(1):187–9.
12. Kiyama H, Kakizawa S, Sasajima Y, Tahara YO, Miyata M. Reconstitution of a minimal motility system based on *Spiroplasma* swimming by two bacterial actins in a synthetic minimal bacterium. Sci Adv. 2022;8(48):eabo7490.
13. Liu P, Zheng H, Meng Q, Terahara N, Gu W, Wang S, et al. Chemotaxis without Conventional two-component system, based on cell polarity and aerobic conditions in helicity-switching swimming of *Spiroplasma eriocheiris*. Front Microbiol. 2017;8:58.
14. Fink G, Szewczak-Harris A, Löwe J, SnapShot. Bacterial Cytoskeleton Cell. 2016;166(2):522–e1.
15. van den Ent F, Johnson CM, Persons L, de Boer P, Löwe J. Bacterial actin MreB assembles in complex with cell shape protein RodZ. EMBO J. 2010;29(6):1081–90.
16. Ku C, Lo WS, Kuo CH. Molecular evolution of the actin-like MreB protein gene family in wall-less bacteria. Biochem Biophys Res Commun. 2014;446(4):927–32.
17. Takahashi D, Fujiwara I, Miyata M. Phylogenetic origin and sequence features of MreB from the wall-less swimming bacteria *Spiroplasma*. Biochem Biophys Res Commun. 2020;533(4):638–44.
18. Lartigue C, Lambert B, Rideau F, Dahan Y, Decossas M, Hillion M, et al. Cytoskeletal components can turn wall-less spherical bacteria into kinking helices. Nat Commun. 2022;13(1):6930.
19. Masson F, Pierrat X, Lemaitre B, Persat A. The wall-less bacterium *Spiroplasma poulsonii* builds a polymeric cytoskeleton composed of interacting MreB isoforms. iScience. 2021;24(12):103458.
20. Cisak E, Wójcik-Fatla A, Zając V, Sawczyn A, Sroka J, Dutkiewicz J. *Spiroplasma* - an emerging arthropod-borne pathogen? Annals Agricultural Environ Medicine: AAEM. 2015;22(4):589–93.
21. Trachtenberg S. The cytoskeleton of *spiroplasma*: a complex linear motor. J Mol Microbiol Biotechnol. 2006;11(3–5):265–83.
22. Trachtenberg S, Schuck P, Phillips TM, Andrews SB, Leapman RD. A structural framework for a near-minimal form of life: mass and compositional analysis of the helical mollicute *Spiroplasma melliferum* BC3. PloS one. 2014;9(2):e87921.
23. Iwai N, Nagai K, Wachi M. Novel S-benzylisothiourea compound that induces spherical cells in *Escherichia coli* probably by acting on a rod-shape-determining protein(s) other than penicillin-binding protein 2. Biosci Biotechnol Biochem. 2002;66(12):2658–62.
24. Wachi M, Iwai N, Kunihisa A, Nagai K. Irregular nuclear localization and anucleate cell production in *Escherichia coli* induced by a Ca^{2+} chelator, EGTA. Biochimie. 1999;81(8–9):909–13.
25. Bonez PC, Ramos AP, Nascimento K, Copetti PM, Souza ME, Rossi GG, et al. Antibacterial, cyto and genotoxic activities of A22 compound ((S-3, 4 -dichlorobenzyl) isothiourea hydrochloride). Microb Pathog. 2016;99:14–8.
26. Bean GJ, Flickinger ST, Westler WM, McCully ME, Sept D, Weibel DB, et al. A22 disrupts the bacterial actin cytoskeleton by directly binding and inducing a low-affinity state in MreB. Biochemistry. 2009;48(22):4852–7.
27. Iwai N, Ebata T, Nagura H, Kitazume T, Nagai K, Wachi M. Structure-activity relationship of S-benzylisothiourea derivatives to induce spherical cells in *Escherichia coli*. Biosci Biotechnol Biochem. 2004;68(11):2265–9.
28. Iwai N, Fujii T, Nagura H, Wachi M, Kitazume T. Structure-activity relationship study of the bacterial actin-like protein MreB inhibitors: effects of substitution of benzyl group in S-benzylisothiourea. Biosci Biotechnol Biochem. 2007;71(1):246–8.
29. Lim CH, Song IS, Lee J, Lee MS, Cho YY, Lee JY, et al. Toxicokinetics and tissue distribution of phalloidin in mice. Food Chem Toxicology: Int J Published Br Industrial Biol Res Association. 2023;179:113994.
30. Cooper JA. Effects of cytochalasin and phalloidin on actin. J Cell Biol. 1987;105(4):1473–8.
31. Stemke GW, Robertson JA. Comparison of two methods for enumeration of mycoplasmas. J Clin Microbiol. 1982;16(5):959–61.
32. Danxia Zhou RW, Kang Xin Z, Qian Y, Ji HY. Cloning and expression of cytoskeleton-related gene mreB and expression differences between two shapes of *Spiroplasma melliferum*. Microbiol China. 2014;41(9):1771–8.

33. Harne S, Duret S, Pande V, Bapat M, Béven L, Gayathri P. MreB5 is a determinant of rod-to-helical transition in the cell-wall-less bacterium *Spiroplasma*. Curr Biology: CB. 2020;30(23):4753–e627.
34. Harne S, Gayathri P. Characterization of heterologously expressed Fibril, a shape and motility determining cytoskeletal protein of the helical bacterium *Spiroplasma*. iScience. 2022;25(10):105055.
35. Takahashi D, Miyata M, Fujiwara I. Assembly properties of bacterial actin MreB involved in *Spiroplasma* swimming motility. J Biol Chem. 2023;299(6):104793.
36. Takahashi D, Fujiwara I, Sasajima Y, Narita A, Imada K, Miyata M. ATP-dependent polymerization dynamics of bacterial actin proteins involved in *Spiroplasma* swimming. Open Biology. 2022;12(10):220083.
37. Sasajima Y, Kato T, Miyata T, Kawamoto A, Namba K, Miyata M. Isolation and structure of the fibril protein, a major component of the internal ribbon for *Spiroplasma* swimming. Front Microbiol. 2022;13:1004601.
38. Takahashi D, Miyata M. Sequence analyses of a lipoprotein conserved with bacterial actins responsible for swimming motility of wall-less helical *Spiroplasma*. microPublication biology. 2023;2023.
39. Awuni E, Mu Y. Effect of A22 on the conformation of bacterial actin MreB. Int J Mol Sci. 2019;20(6).
40. Wang W, Gu Z. Rickettsia-like organism associated with tremor disease and mortality of the Chinese mitten crab *Eriocheir sinensis*. Dis Aquat Organ. 2002;48(2):149–53.
41. Wei P, Ning M, Yuan M, Li X, Shi H, Gu W et al. *Spiroplasma eriocheiris* enters *Drosophila Schneider 2* cells and relies on clathrin-mediated endocytosis and Macropinocytosis. Infect Immun. 2019;87(11).
42. Hou L, Gu W, Zhu H, Yao W, Wang W, Meng Q. *Spiroplasma eriocheiris* induces mouse 3T6-Swiss albino cell apoptosis that associated with the infection mechanism. Mol Immunol. 2017;91:75–85.
43. Gu W, Yao W, Zhao Y, Pei S, Jiang C, Meng Q, et al. Establishment of *spiroplasma*-infected hemocytes as an in vitro laboratory culture model of Chinese mitten crab *Eriocheir sinensis*. Vet Microbiol. 2014;171(1–2):215–20.
44. Wieland T, Faulstich H. Amatoxins, phallotoxins, phallolysin, and antamanide: the biologically active components of poisonous Amanita mushrooms. CRC Crit Reviews Biochem. 1978;5(3):185–260.
45. Loranger A, Tuchweber B, Gicquaud C, St-Pierre S, Côté MG. Toxicity of peptides of Amanita virosa mushrooms in mice. Fundamental Appl Toxicology: Official J Soc Toxicol. 1985;5(6 Pt 1):1144–52.
46. Mengs U, Trost W. Acute phalloidin poisoning in dogs. Arch Toxicol. 1981;48(1):61–7.
47. Tuchweber B, Sieck R, Trost W. Prevention of silybin of phalloidin-induced acute hepatoxicity. Toxicol Appl Pharmcol. 1979;51(2):265–75.
48. Chen Y, Wei D, Wang Y, Zhang X. The role of interactions between bacterial chaperone, aspartate aminotransferase, and viral protein during virus infection in high temperature environment: the interactions between bacterium and virus proteins. BMC Microbiol. 2013;13:48.
49. Singhi D, Srivastava P. Role of bacterial cytoskeleton and other apparatuses in Cell Communication. Front Mol Biosci. 2020;7:158.
50. Jin M, Chen Y, Xu C, Zhang X. The effect of inhibition of host MreB on the infection of thermophilic phage *GVE2* in high temperature environment. Sci Rep. 2014;4:4823.
51. Noguchi N, Yanagimoto K, Nakaminami H, Wakabayashi M, Iwai N, Wachi M, et al. Anti-infectious effect of S-benzylisothiourea compound A22, which inhibits the actin-like protein, MreB, in Shigella flexneri. Biol Pharm Bull. 2008;31(7):1327–32.
52. Ranjit DK, Liechti GW, Maurelli AT. Chlamydial MreB directs Cell Division and Peptidoglycan Synthesis in *Escherichia coli* in the absence of FtsZ activity. mBio. 2020;11(1).
53. Takahashi D, Fujiwara I, Miyata M. Purification and ATPase activity measurement of *Spiroplasma* MreB. Methods in molecular biology. (Clifton NJ). 2023;2646:359–71.

Publisher's note